INTERNATIONAL JOURNAL OF OPTIMIZATION IN CIVIL ENGINEERING
Int. J. Optim. Civil Eng., 2019; 9(3):437-455

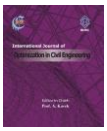

FRAGILITY CURVES FOR STRUCTURES EQUIPPED WITH OPTIMAL SATMDs

S. Bakhshinezhad and M. Mohebbi[*, †]
Faculty of Engineering, University of Mohaghegh Ardabili, 56199-11367, Ardabil, Iran

ABSTRACT

In this paper, a procedure has been presented to develop fragility curves of structures equipped with optimal variable damping or stiffness semi-active tuned mass dampers (SATMDs). To determine proper variable damping or stiffness of semi-active devices in each time step, instantaneous optimal control algorithm with clipped control concept has been used. Optimal SATMDs have been designed based on minimization of maximum inter-story drift of nonlinear structure which genetic algorithm(GA) has been used to solve the optimization problem. For numerical analysis, a nonlinear eight-story shear building with bilinear hysteresis material behavior has been used. Fragility curves for the structure equipped with optimal variable damping and stiffness SATMDs have been developed for different performance levels and compared with that of uncontrolled structure as well as structure controlled using passive TMD. Numerical analysis has shown that for most range of intensity measure optimal SATMDs have been effective in enhancement of the seismic fragility of the nonlinear structures which the improvement has been more than passive TMDs. Also, it has been found that, although variable stiffness SATMD shows to be more reliable in lower mass ratios, however in higher mass ratios variable stiffness and damping SATMDs performs similarly to improve reliability of the structure.

Keywords: fragility curves; reliability assessment; semi - active tuned mass dampers; variable damping SATMD; variable stiffness SATMD; genetic algorithm.

Received: 12 October 2018; Accepted: 20 February 2019

1. INTRODUCTION

Tuned Mass Damper (TMD) is a passive structural control mechanism that absorbs seismic energy by oscillating under dynamic loads such as earthquakes and winds. Effectiveness of

[*]Corresponding author: Faculty of Engineering, University of Mohaghegh Ardabili, 56199-11367, Ardabil, Iran
[†]E-mail address: mohebbi@uma.ac.ir (M. Mohebbi)

TMD in structural response reduction has led to pay much attention during past years and even implementation in many actual buildings [1-3]. TMD consists of a mass, spring and damper which is usually installed at the top floor of buildings. Due to the fact that TMD should be tuned to a fixed frequency, it may have no benefits during some earthquakes which induce the structure to vibrate in other frequency bands. Furthermore, under severe earthquakes, the structure undergoes nonlinear behavior which may detune the TMD and consequently will lead to inefficiency. Recently, the semi-active tuned mass damper (SATMD) with variable damping [4] or variable stiffness [5] has been proposed to overcome the disadvantageous of conventional TMDs. Many studies have focused on the performance assessment and optimal design of SATMDs for linear and nonlinear structures in a deterministic manner [6].

However, loading uncertainties caused by random nature of earthquakes could heavily affect the efficiency of SATMDs. Thus, the uncertainties in applied excitation should be considered in assessing the performance of SATMDs in a probabilistic framework. A systematic way to probabilistic analysis and reliability assessment of structures dealing with randomness of the input excitation is development of fragility curves. Fragility curves represent the conditional probability of being in or exceeding some performance limit states capacity over prescribed intensity measure. Seismic fragility analysis was first used for safety assessment of nuclear power plants. In the following, it has extended especially for bridges and buildings [7].

During past decade, many investigations have been done on developing fragility curves for structures equipped with control systems such as passive, active and semi-active mechanisms. Some researchers have developed fragility curves of structures equipped with passive control systems. Castaldo et al. [8] have developed fragility curves for a linear base isolated structure which structure and isolation parameters uncertainties have been considered by using uniform random numbers. Incremental Dynamic Analysis (IDA) has been conducted using generated artificial earthquakes and fragility has been calculated for each intensity measure. Wilbee et al. [9] have developed fragility curves for a nonlinear benchmark building equipped with MR dampers with constant voltage as passive devices. Wong and Harris [10] have developed fragility curves for a nonlinear frame equipped with TMD on the top floor. TMDs with different mass ratios have been considered and Incremental Dynamic Analysis has been performed on the structure by using artificial earthquake records. Results have illustrated that installing TMD has the ability to improve seismic fragility of the structure. In some researches, the effectiveness of active and semi-active control systems in fragility improvement have been studied. Taylor [11] has developed fragility curves of nonlinear structures equipped with passive dampers and active controllers and studied the effect of placement of control systems. Barnawi [12], has evaluated fragility relationships of a nonlinear structure equipped with passive, active and semi-active mechanisms. Magnetorheological (MR) dampers have been used as passive and semi-active as well as ideal actuators as active control systems. In a similar study, Barnawi and Dyke [13], have investigated the performance of passive and semi-active MR dampers and ideal active controllers in mitigating the fragility of the nonlinear structures. Cha and Bai [14], have studied the effectiveness of semi-active MR dampers in fragility of high-rise structures. As a result of all studies, it has been found that semi-active control systems have the capability of reducing fragility of the structures more effective than passive and active

control systems. In previous studies, there is no study in the field of fragility curves of structures equipped with SATMDs. Due to the capabilities of SATMDs with variable damping and stiffness and their superiority than TMDs especially for control of nonlinear structures, in this paper, it has been focused on fragility curves of optimal SATMD controlled structures.

In this paper, a procedure to develop fragility curves for structures equipped with variable damping and stiffness SATMDs has been presented. SATMDs with different mass ratios based on instantaneous optimal control and clipped control concept have been designed for a nonlinear shear building using an optimization technic. Fragility curves have been developed and performance of optimal variable damping and stiffness SATMDs in reducing seismic fragility have been investigated and compared with fragility curves of uncontrolled structure and equipped with passive TMDs.

2. FRAGILITY CURVES

Fragility represents the conditional probability of being in or exceeding some performance limit state capacities by structural demand responses over prescribed intensity measure. Mathematic formulation of fragility is defined as follows:

$$F = P\left[R \geq R_{LS} \,|\, IM\right] \tag{1}$$

where R is the response of the structure such as displacement, drift, acceleration and etc., R_{LS} is the limit state capacity related to the response R and IM is the intensity measure of the input excitation. The limit state function is defined as:

$$g = R_{LS} - R \tag{2}$$

which means if g>0, structural performance is acceptable and the structure is safe. Else, g≤0 structural performance is not acceptable and the structure is failed. By assuming lognormal distribution for response R and by assuming limit state capacity R_{LS} as a deterministic threshold from code requirements, the fragility relationship can be derived by the following equation [12]:

$$F = 1 - \Phi\left(\frac{\ln(R_{LS}) - \lambda_{R|IM}}{\beta_T}\right) \tag{3}$$

where Φ is standard normal cumulative distribution function. $\lambda_{R|IM}$ is natural logarithm of median of the response in a specific intensity measure which is determined based on the estimated relationship between intensity measure and response of the structure. β_T is total uncertainty of the system consisted of demand, capacity and modeling uncertainties as follows:

$$\beta_T = \sqrt{\beta_{R|IM}{}^2 + \beta_{R_{LS}}{}^2 + \beta_M{}^2} \tag{4}$$

Demand uncertainty, $\beta_{R|IM}$, is as:

$$\beta_{R|IM} = \sqrt{Ln(1+S^2)} \tag{5}$$

where s^2 is standard error as:

$$S^2 = \sum \left(Ln(R_i) - Ln(R_p)\right)^2 / n-2 \tag{6}$$

In this equation, R_i and R_P are observed and predicted response of the structure respectively. n is the number of response sample data. $\beta_{R_{LS}}$ and β_M are capacity and modeling uncertainties, which the value of 30% is a reasonable choice for them [12].

2.1 Relationship between response and intensity measure

The relationship between the intensity measure (*IM*) and response (*R*) can be determined by power-law model [12] or IDA curves. In this paper, the power-law model procedure has been used as follows:

$$R = a\ (IM)^b \tag{7}$$

By logarithmic transformation of Equation (8), the linear form can be derived as:

$$\ln(R) = \ln(a) + b.\ln(IM) \tag{8}$$

A linear regression analysis can be used to find unknown constants of *a* and *b*. Different intensity measures such as Peak Ground Acceleration (PGA), Peak Ground Velocity (PGV), spectral acceleration (S_a), spectral displacement (S_d) and etc could be used for the fragility analysis. In this research, S_a has been considered as earthquake intensity measure.

2.2 Limit state capacity

Several limit states have been used based on various responses of structure subjected to earthquake, but specific code guidelines to choose appropriate limit state thresholds are limited. FEMA356 recommends using inter-story drift ratio (θ) to identify structural performance levels. Inter-story drift ratio is the ratio of the relative displacement between the successive stories and the story height. In this research, limit state of maximum inter-story drift ratio as safety criterion has been used to seismic fragility analysis of structure by following FEMA guideline for performance levels, i.e. Immediate Occupancy (IO), Life Safety (LS) and Collapse Prevention (CP) according to Table 1.

Table 1: limit state capacities considered for fragility analysis

Performance levels	Inter-story drift ratio
Immediate Occupancy	0.007
Life Safety	0.025
Collapse Prevention	0.05

3. VARIABLE DAMPING AND STIFFNESS SATMD

In this paper, optimal variable damping SATMD (SATMD-VD) and variable stiffness SATMD (SATMD-VS) with different mass ratios have been designed for the nonlinear structure. Instantaneous optimal control algorithm with clipped control law has been used to determine the proper damping or stiffness of the semi-active devices in each time step. Optimal properties of the semi-active control system have been designed based on defining an optimization problem to minimize maximum inter-story drift of the structure and have been solved by genetic algorithm (GA).

3.1 SATMD-structure equation of motion

The equation of motion of the nonlinear *n* story shear building frame equipped with a SATMD installed on its top subjected to ground acceleration $\ddot{X}_g$ is as follows:

$$\mathbf{M}\ddot{\mathbf{X}}(t)+\mathbf{F}_D\left(\dot{\mathbf{X}}(t)\right)+\mathbf{F}_S\left(\mathbf{X}(t)\right)=\mathbf{D}u_{SA}(t)+\mathbf{Me}\ddot{X}_g \tag{9}$$

$X(x_1,x_2,...,x_n,x_{satmd})$, $\dot{X}(\dot{x}_1,\dot{x}_2,...,\dot{x}_n,\dot{x}_{satmd})$ and $\ddot{X}(\ddot{x}_1,\ddot{x}_2,...,\ddot{x}_n,\ddot{x}_{satmd})$ are displacement, velocity and acceleration vectors of the SATMD-structure system with respect to the ground, respectively. $e^T=[-1,-1,...,-1]_{1\times(n+1)}$ is ground acceleration-mass transformation vector. *M* is the diagonal mass matrix as follows:

$$\mathbf{M}=\begin{bmatrix} m_1 & 0 & \cdots & 0 & 0 \\ 0 & m_2 & \cdots & 0 & 0 \\ \vdots & \vdots & \ddots & \vdots & \vdots \\ 0 & 0 & \cdots & m_n & 0 \\ 0 & 0 & \cdots & 0 & m_{satmd} \end{bmatrix}_{(n+1)\times(n+1)} \tag{10}$$

F_D and F_S are vectors of damping and restoring force which are functions of velocity and displacement [15], respectively. $D^T=[0,0,...,1,-1]_{1\times(n+1)}$ is the location matrix of semi-active device and u_{SA} is the semi-active control force applied between mass damper and the top floor of the structure. In case of variable damping SATMD which is constructed by substituting conventional damper of TMD with a semi-active device such as semi-active fluid viscous damper [4], u_{SA} is as follows:

$$u_{SA}(t) = c_d(t) \times \dot{x}_{damper} \tag{11}$$

which, $\dot{x}_{damper}$ is the velocity of mass damper with respect to the top floor. c_d is variable damping coefficient of the SATMD which is determined by the control algorithm in each time step. On the other hand, Variable stiffness SATMD is constructed by substituting conventional spring of TMD with a semi-active device such as SAIVS [5] and semi-active control force is as follows:

$$u_{SA}(t) = k_d(t) \times x_{spring} \tag{12}$$

which x_{spring} is the displacement of mass damper with respect to the top floor. k_d is variable stiffness of the SATMD and is determined by the control algorithm. The Newmark integration method [16] has been used to solve equation of motion of the structure.

3.2 Instataneous optimal control algorithm and clipped control law

The semi-active control law is consisted of two stages. The first one is determining active control force based on instantaneous optimal control algorithm which is developed for the nonlinear structures [15], by the following equation:

$$u_{active}(t) = -\mathbf{R}^{-1}\mathbf{D}^T\mathbf{K}_n^{*-T}(t)\left(\mathbf{Q}_1\mathbf{X}(t) + a_4\mathbf{Q}_2\dot{\mathbf{X}}(t) + a_1\mathbf{Q}_3\ddot{\mathbf{X}}(t)\right) \tag{13}$$

Q_1, Q_2 and Q_3 are $(n+1)\times(n+1)$ positive semi-definite weighting matrices corresponding to the penalty of structural responses. R is a matrix corresponds to penalty of the control force which is a scalar in case of SATMD with one controller. $\mathbf{K}_n^*$ is generalized stiffness matrix which in time step k is:

$$\mathbf{K}_{n_k}^* = a_1\mathbf{M} + a_4\mathbf{C}_{k-1}^* + \mathbf{K}_{k-1}^* \tag{14}$$

$\mathbf{C}_{k-1}^*$ and $\mathbf{K}_{k-1}^*$ are the nonlinear damping and stiffness matrices at time step k-1. a_1 and a_4 are the coefficients of Newmark's numerical integration method [15].

In the second stage, based on clipped control law the properties of semi-active devices adjust such that the most similar control force to the ideal active control force be generated and applied to the structure. In case of variable damping SATMD, the damping coefficient in each time step is calculated as follows:

$$c_d(t) = \begin{cases} c_{\min} & u_{active}/\dot{x}_{damper} \le c_{\min} \\ u_{active}/\dot{x}_{damper} & c_{\min} < u_{active}/\dot{x}_{damper} < c_{\max} \\ c_{\max} & u_{active}/\dot{x}_{damper} \ge c_{\max} \end{cases} \tag{15}$$

Similarly, for variable stiffness SATMD, the stiffness is calculated as follows:

$$k_d(t)=\begin{cases}k_{\min} & u_{active}/x_{spring}\le k_{\min}\\ u_{active}/x_{spring} & k_{\min}<u_{active}/x_{spring}<k_{\max}\\ k_{\max} & u_{active}/x_{spring}\ge k_{\max}\end{cases} \tag{16}$$

4. OPTIMAL DESIGN OF SATMDS

A procedure has been used to design variable damping SATMDs as well as variable stiffness SATMDs using an optimization technic. In this method which has been proposed previously for designing active mass damper systems [15] and active tendon control systems [17], parameters of weighting matrices Q_1, Q_2 and Q_3 of the control force applied to the nonlinear structure according to equation (13), are considered as design variables. Herein, for SATMD system the upper and lower bound of semi-active damping or stiffness devices are also considered as design variables. In most of previous researches on designing control systems, the amount of reduction in maximum inter-story drift of the structure as safety criterion has been used to assess the effectiveness of the structural control system. In this paper, too, minimization of the maximum inter-story drift of the structure has been considered as objective function. In practice, due to limited space available for SATMD installation, the maximum stroke length should be limited in design and implementation process of SATMDs. Thus, the optimization problem with the objective function of minimization of maximum inter-story drift with constrain on SATMD stroke length has been defined as the following equation.

$$\begin{array}{lll}\textit{Find}: & Q_1,Q_2,Q_3,c_{\min},c_{\max} \quad \textit{or} \quad Q_1,Q_2,Q_3,k_{\min},k_{\max} & \\ \textit{Minimize}: & d_{\max}=\max\left(\left|drift_i(k)\right|\right), \quad k=1,2,\ldots,k_{\max}, \quad i=1,2,\ldots,n & \\ \textit{Subject to}: & d_{\max,SATMD}\le U_L & \end{array} \tag{17}$$

where k_{max} is total number of time steps and $drift_i(k)$ is inter-story drift of the ith story at time step k. U_L is the maximum acceptable stroke length of SATMD which can be defined by the designer considering practical limitations. The arrangement for weighting matrices has been considered as follows [15]:

$$Q_1=\begin{bmatrix}q_1[I]_{n\times n} & [0]_{n\times 1}\\ [0]_{1\times n} & q_{1m}\end{bmatrix}_{(n+1)\times(n+1)} \tag{18}$$

$$Q_2=\begin{bmatrix}q_2[I]_{n\times n} & [0]_{n\times 1}\\ [0]_{1\times n} & q_{2m}\end{bmatrix}_{(n+1)\times(n+1)} \tag{19}$$

$$Q_3=\begin{bmatrix}q_3[I]_{n\times n} & [0]_{n\times 1}\\ [0]_{1\times n} & q_{3m}\end{bmatrix}_{(n+1)\times(n+1)} \tag{20}$$

where *[I]* is unit matrix and *[0]* is zero matrix. Each weighting matrix has two parameters. So, there are eight design variables for SATMDs. The constrained optimization problem was

reformulated as an unconstrained optimization problem by adding a penalty term for violation of constrain to the objective function. The optimization problem is as follows:

$$\begin{aligned} &\textit{Find}: && q_1, q_2, q_3, q_{1m}, q_{2m}, q_{3m}, c_{\min}, c_{\max} \quad \textit{or} \quad q_1, q_2, q_3, q_{1m}, q_{2m}, q_{3m}, k_{\min}, k_{\max} \\ &\textit{Minimize}: && d_{\max} + \beta.\max[0, g_1] \\ & && g_1 = \frac{d_{\max}(satmd)}{U_L} - 1 \end{aligned} \tag{21}$$

where β is penalty coefficient and has been selected as $\beta=200$.

4.1 Solving the optimization problem using GA

Genetic algorithm (GA) is one of the most effective optimization methods which has been presented first by Holland [18] and has been inspired by the evolution process in nature. It has been extensively used in engineering application as well as civil engineering [19-21] and also structural control system design [22-24], because of its simplicity and capability for solving nonlinear optimization problems with large number of design variables. GA has three main operations including selection, crossover and mutation [25]. In this study, the stochastic universal sampling [26] has been used for selecting the individuals for mating, where the probability of selecting an individual is as follows:

$$P(x_i) = \frac{F(x_i)}{\sum_{i=1}^{N_{ind}} F(x_i)} \tag{22}$$

where $F(x_i)$ is the fitness of chromosome x_i, $P(x_i)$ is the probability of selecting x_i and N_{ind} is the number of individuals. The selected chromosomes are then chosen through crossover operator to generate newborns. The intermediate recombination method [27] has been used for crossover, where newborns are produced based on linear combination of parent genes as follows:

$$G_{1,2} = P_1 + \alpha(P_2 - P_1) \tag{23}$$

where G_1 and G_2 are the newborn chromosome genes, P_1 and P_2 are the corresponding parent chromosome genes and α is a scale factor that is selected randomly over [-0.25, 1.25] in order to produce newborn genes. Mutation operator in GA algorithm has been used to avoid local minima and to ensure searching all individuals. The number of mutated individuals is calculated from:

$$N_{mutated} = m_r.N_{new}.N_{\text{var}} \tag{24}$$

where m_r is the mutation rate which has been suggested to be a small number and in this paper has been chosen to be 0.04. N_{new} and N_{var} are the number of newborns and variables in each generation, respectively.

5. NUMERICAL ANALYSIS AND DISCUSSION

In this section, the methodology of developing fragility curves for structure equipped with variable damping and stiffness SATMDs has been presented through numerical analysis. Optimal SATMDs with different mass ratios have been designed for the nonlinear structure with objective of minimization of maximum inter-story drift. SATMDs have been installed on the top of an eight-story nonlinear shear building frame as shown in Fig. 1. The nonlinear behavior of the structure has been assumed as bilinear hysteretic model shown in Fig. 2. The elastic stiffness is $K_1=3.404\times10^5 kN/m$ and post-elastic stiffness is $K_2=3.404\times10^4 kN/m$. All characteristics are similar for all stories. The story mass is $m=245.6ton$ and linear viscous damping coefficient is $c=734.3kN.s/m$. Story height is $3.2m$ and Yielding inter-story drift is $u_y=2.4cm$. Fundamental period of the structure based on its initial stiffness is $T_1=1.087s$.

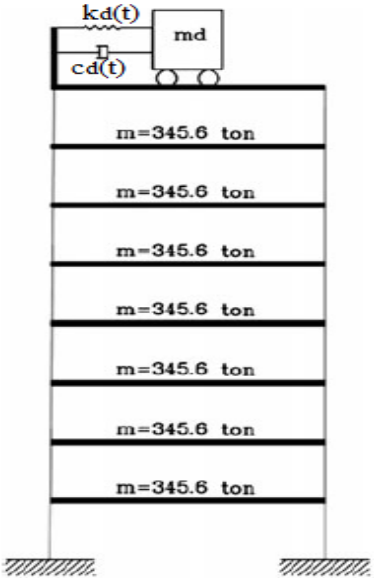

Figure 1. SATMD-structure model

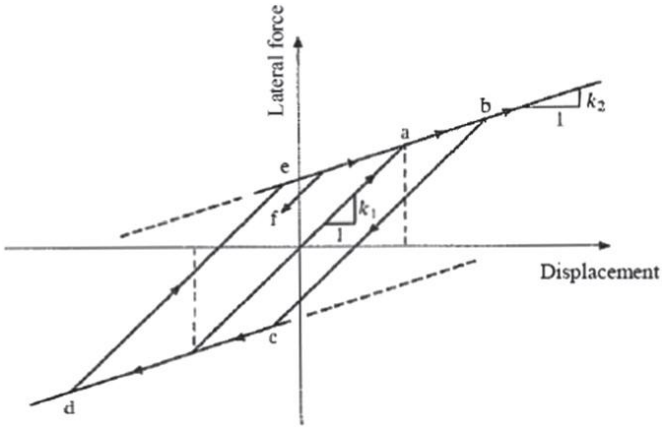

Figure 2. Bilinear elastic-plastic stiffness model

5.1 Ground motions

Loading uncertainty is one of the most important issues which could have heavy effect on structural performance. Because of the inherent random nature of earthquakes, the structure may be subjected to any ground motion which has its unique properties. In fragility analysis, this uncertainty is taken into consideration by using a set of different earthquakes with different intensities. There are no clear code guidelines about required number of records for fragility analysis, but about twenty records could be enough to assess seismic demand accurately. A set of 10 pairs of earthquakes with probability of occurrence of 10% in 50 years proposed for SAC project and recommended in ASCE/SEI-7-05 design code for downtown Los Angeles have been used for fragility analysis which their properties has been presented in Table 2. It has been assumed that the structure to be located on stiff soil which corresponds to site class D based on this code. The f_n component of the Imperial Valley 1940, El Centro earthquake which shows most compatibility to the design spectrum than other earthquakes, has been selected as the design record, where its acceleration time history has been shown in Fig. 3. Fig. 4 shows the acceleration response spectrum of the selected earthquakes, design record and ASCE design spectrum.

Table 2: Selected earthquake records used in current study

Earthquake code	Earthquake name	Year	Staion	Magnitude	Distance (km)	PGA (g)	$S_a(T_1,\xi=5\%)$ (g)
La01	Imperial Valley-f_n	1940	El Centro	6.9	10.0	0.46	0.58
La02	Imperial Valley-f_p	1940	El Centro	6.9	10.0	0.68	0.87
La03	Imperial Valley-f_n	1979	Array #05	6.5	4.1	0.39	0.69
La04	Imperial Valley-f_p	1979	Array #05	6.5	4.1	0.49	0.39
La05	Imperial Valley-f_n	1979	Array #06	6.5	1.2	0.30	0.40
La06	Imperial Valley-f_p	1979	Array #06	6.5	1.2	0.23	0.31
La07	Landers-f_n	1992	Barstow	7.3	36.0	0.42	0.52
La08	Landers-f_p	1992	Barstow	7.3	36.0	0.43	0.63
La09	Landers-f_n	1992	Yermo	7.3	25.0	0.52	0.85
La10	Landers-f_p	1992	Yermo	7.3	25.0	0.36	0.76
La11	Loma Prieta-f_n	1989	Gilroy	7.0	12.0	0.67	0.71
La12	Loma Prieta-f_p	1989	Gilroy	7.0	12.0	0.97	0.36
La13	Northridge-f_n	1994	Newhall	6.7	6.7	0.68	0.91
La14	Northridge-f_p	1994	Newhall	6.7	6.7	0.66	1.08
La15	Northridge-f_n	1994	Rinaldi RS	6.7	7.5	0.53	0.93
La16	Northridge-f_p	1994	Rinaldi RS	6.7	7.5	0.58	1.16
La17	Northridge-f_n	1994	Sylmar	6.7	6.4	0.57	0.47
La18	Northridge-f_p	1994	Sylmar	6.7	6.4	0.82	0.82
La19	North Palm Springs-f_n	1986	-	6.0	6.7	1.02	0.49
La20	North Palm Springs-f_p	1986	-	6.0	6.7	0.99	1.05

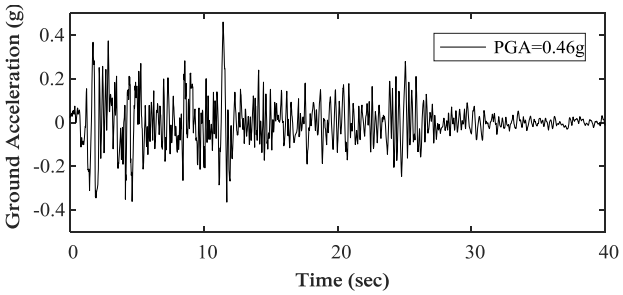

Figure 3. Time history of ground acceleration of the design record

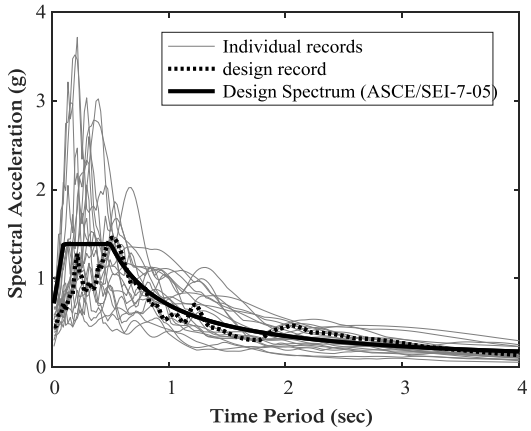

Figure 4. Acceleration response spectrum of the selected and design earthquake records and the design response spectrum at downtown Los Angeles for site class D

5.2 Optimal design of SATMDs using GA

In this section, variable damping SATMDs as well as variable stiffness SATMDs with mass ratio of μ=1%,5%,10%,15% installed at top floor of the considered nonlinear shear building has been designed based on an optimization technic using GA. The properties of the TMDs including mass, stiffness and damping have been designed based on Sadeck et al. [28] procedure according to Table 3 and have been used to design SATMDs.

Table 3: Optimum parameters of TMDs

Mass ratio μ(%)	m_{tmd} (ton)	k_{tmd} (kN/m)	c_{tmd} (kN.s/m)
1	23.676	773.478	35.739
5	118.379	3503.623	363.084
10	236.759	6237.180	940.360
15	355.138	8382.565	1594.505

Each SATMD has 8 design variables including parameters of weighting matrices q_1, q_2, q_3, q_{1m}, q_{2m}, q_{3m} as well as upper and lower limit of semi-active device where in case of variable damping SATMD are c_{min} and c_{max} and in case of variable stiffness SATMD are k_{min} and k_{max}. For different values of SATMD mass ratio and both variable damping and stiffness semi-active strategies, the optimization problem defined in equation (21) with the objective

of minimization of maximum inter-story drift of the structure under design record with constrain on SATMD stroke length equal to U_L=1.0m has been solved frequently by GA. The parameters of the GA have been chosen as presented in Table 4. To ensure the accuracy of the optimization procedure, at least four different runs of GA with different initial population have been conducted for the considered optimization problem.

Table 4: Parameters of genetic algorithm

N_{ind}	Number of individuals in each generation	50
N_{elites}	Number of elites	5
m_r	Mutation rate	0.04
N_{max}	Maximum number of generation	200

To show the procedure of solving the optimization problem, the convergence of the GA best objective function value towards the optimum answer, as sample, for variable damping SATMD with mass ratio of μ=15% for four different runs has been reported in Fig. 5. It can be observed that all four runs have led to approximately the same optimum answer while the convergence speeds were different. Also, Fig. 6 shows the fitness value of individuals at the final generation for four different runs which shows the same value for most individuals and accuracy of the procedure.

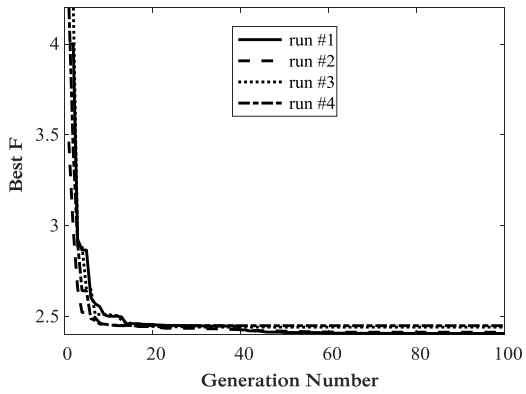

Figure 5. The best objective function for four runs during generations

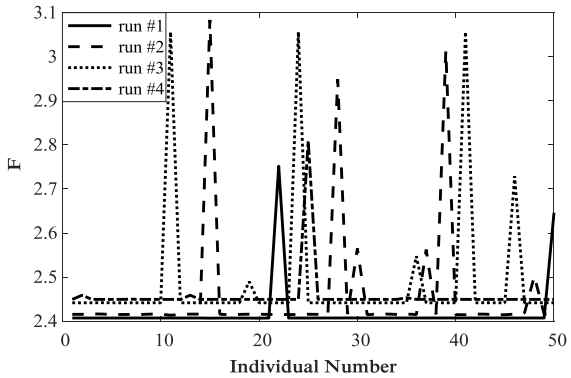

Figure 6. Objective function value at final generation for four runs

Normalized maximum inter-story drift of the structure equipped with optimal SATMDs subjected to the design record has been shown in Fig. 7. In this figure, the responses have been normalized to the maximum drift of the uncontrolled structure. The responses of passive TMDs have also been presented for comparison. It is observed that the performance of SATMDs in reducing maximum drift is more effective than TMDs. As predicted and shown in other studies [2], the response reduction is amplified by increasing the mass ratio of TMD. This phenomenon has also been observed in SATMDs with variable damping and stiffness. However, sensitivity to the mass ratio in SATMD with variable stiffness is less than variable damping and in higher mass ratios the SATMDs show similar performance. Particularly, in mass ratio of μ=15%, SATMD with variable damping and stiffness has reduced maximum drift near to 69% with respect to the uncontrolled structure and about 53% with respect to the TMD controlled structure.

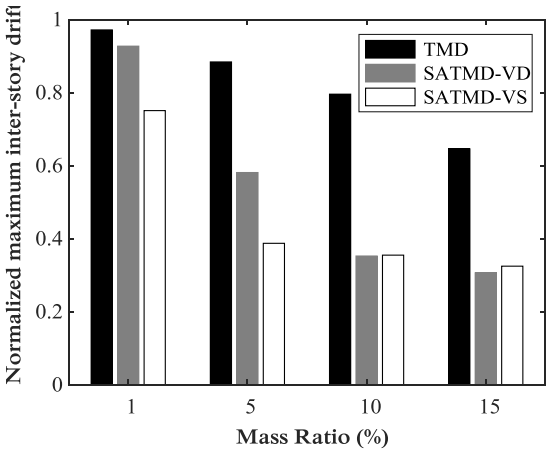

Figure 7. Normalized inter-story drift and of the designed variable damping (VD) and variable stiffness (VS) SATMDs

5.3 Regression analysis

The structure has been subjected to earthquakes and maximum responses of the uncontrolled structure and equipped with TMDs and optimal SATMDs have been derived. These maximum responses under each seismic record are taken as samples to be used for regression analysis. By assuming power-law model according to Equation (7), the relationship between natural logarithm of S_a and natural logarithm of the response of the structure would be linear. Linear regression analysis has been used to identify the properties of these lines such as slope, intercept and correlation. The values of parameters *a* and *b* in power-law model has been calculated with determined slope and intercept of the lines. Fig. 8 and 9 shows observed and estimated maximum inter-story drift ratio of the structure controlled by variable damping and stiffness SATMDs with mass ratio of μ=15%, respectively. The calculated power-law model parameters and demand uncertainty for uncontrolled structure and equipped with TMDs and SATMDs for estimating the relationship between S_a and inter-story drift ratio has been presented in Table 5.

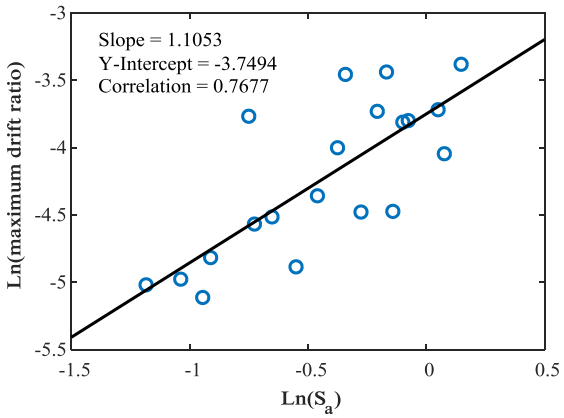

Figure 8. relationship of intensity measure and inter-story drift ratio of variable damping SATMD

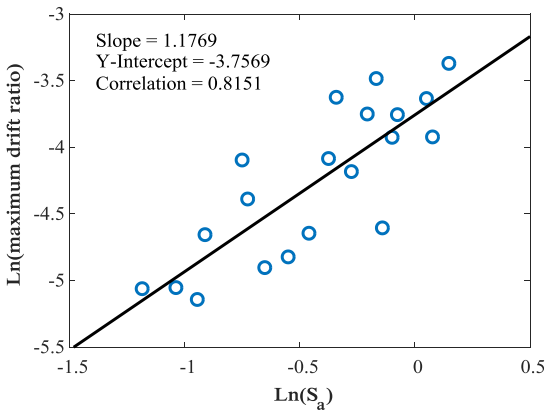

Figure 9. relationship of intensity measure and inter-story drift ratio of variable stiffness SATMD

Table 5: power-law model parameters and demand uncertainty for uncontrolled structure and equipped with TMDs and SATMDs

mechanism	a	b	$\beta_{R\|PGA}$
Uncontrolled	0.0323	0.9291	0.234
TMD(μ=1%)	0.0325	1.0049	0.232
TMD(μ=5%)	0.0311	1.0832	0.262
TMD(μ=10%)	0.0290	1.1250	0.312
TMD(μ=15%)	0.0272	1.1370	0.347
SATMD-VD(μ=1%)	0.0325	1.0434	0.223
SATMD-VD(μ=5%)	0.0292	1.1858	0.309
SATMD-VD(μ=10%)	0.0261	1.1402	0.356
SATMD-VD(μ=15%)	0.0235	1.1053	0.363
SATMD-VS(μ=1%)	0.0316	1.0023	0.267
SATMD-VS(μ=5%)	0.0254	1.1444	0.310
SATMD-VS(μ=10%)	0.0243	1.1158	0.366
SATMD-VS(μ=15%)	0.0234	1.1769	0.331

5.4 Fragility curves of SATMDs

Optimal variable damping and stiffness SATMDs with mass ratios of μ=1%,5%,10%,15% have been used for seismic response control of nonlinear structure. Fragility curves of the structure equipped with SATMDs have been generated according to Equation (3) and compared to fragility curves of the uncontrolled structure and equipped with TMDs. Fig. 10 presents fragility curves of SATMDs with different mass ratios for IO performance level. It is observed that using SATMDs enhances the seismic fragility of the structure especially, for higher mass ratios and enhancement is slightly more effective than passive TMDs. Also, the performance of variable damping and stiffness SATMDs are almost similar in this performance level. Reliability is defined as the complement of the fragility probability at specific intensity measure. SATMDs with mass ratio of μ=15% has increased the reliability with respect to the uncontrolled structure about 20% at Sa=0.5g.

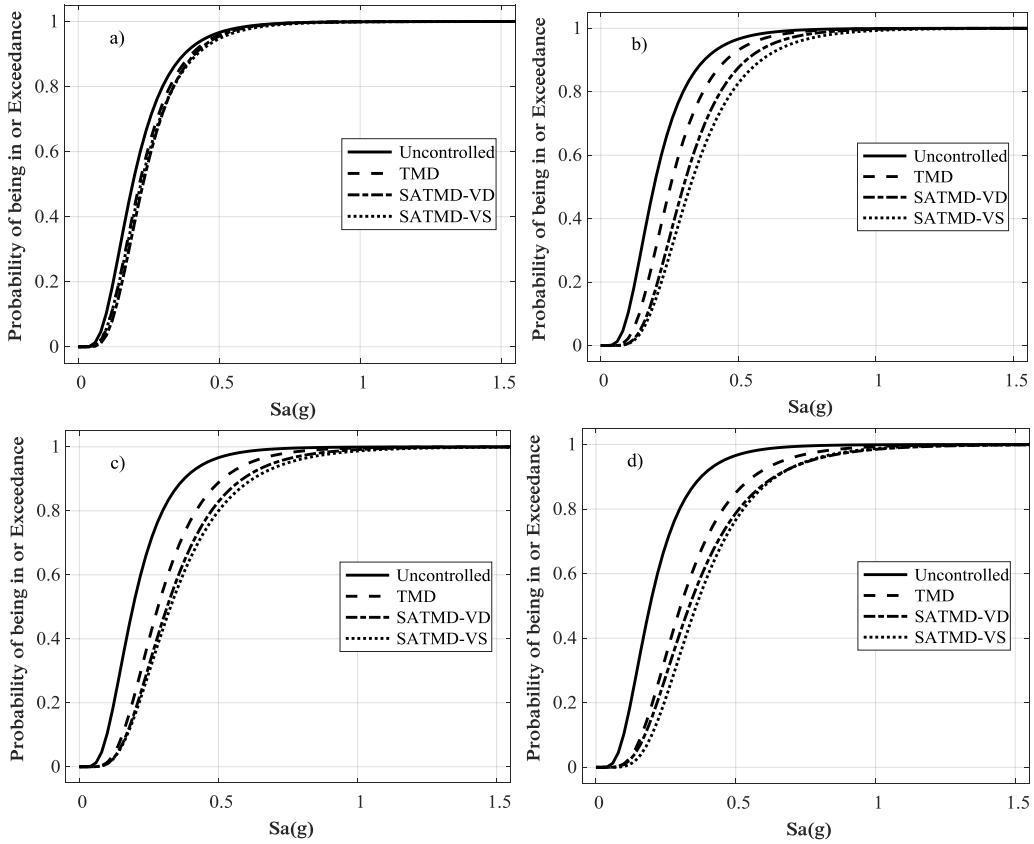

Figure 10. Fragility curves of uncontrolled structure and controlled with TMD and optimal SATMDs with mass ratio of a) μ=1%, b) μ=5%, c) μ=10% and d) μ=15% for IO performance level

Fragility curves of the structure for LS and CP performance levels have been shown in Fig. 11 and 12 respectively. Results show that regardless of performance level, using TMD and SATMDs with mass ratio of μ=1% is ineffective in reducing fragility of the structure. However, for higher mass ratios the SATMDs are effective in mitigating the fragility of the structure.

Comparing variable damping and stiffness SATMDs, it is observed that similar to the design record, fragility curves of SATMD with variable stiffness is less sensitive to the mass ratio than variable damping and by increasing mass ratio they perform similarly. In particular, at LS performance level and intensity measure of S_a=1.0g, variable stiffness SATMD with mass ratio of μ=5%,10%,15% has increased the reliability with respect to the uncontrolled structure about 19%, 22% and 25%, respectively and Also, These reliability improvements for variable damping SATMDs are about 8%, 17% and 24%. At CP performance level and intensity measure of S_a=1.5g, SATMDs with mass ratio of μ=5%,10%,15% has increased the reliability about 11%, 13% and 15% in case of variable stiffness as well as -1%, 8% and 16% in case of variable damping, respectively.

By comparing the performance of SATMDs with their passive counterpart, TMD, it is observed that SATMDs are more reliable than TMDs and have the ability to enhance seismic fragility of the structure especially, under severe earthquakes which the structure undergoes nonlinear behavior and TMDs are practically detuned. Particularly, for LS performance level and intensity measure of S_a=1.0g, variable stiffness SATMD with mass ratio of μ=5%,10%,15% has increased the reliability with respect to the TMD controlled structure about 16%, 13% and 10%, respectively and These enhancements for CP performance level and intensity measure of S_a=1.5g are about 13%, 11% and 9%, respectively.

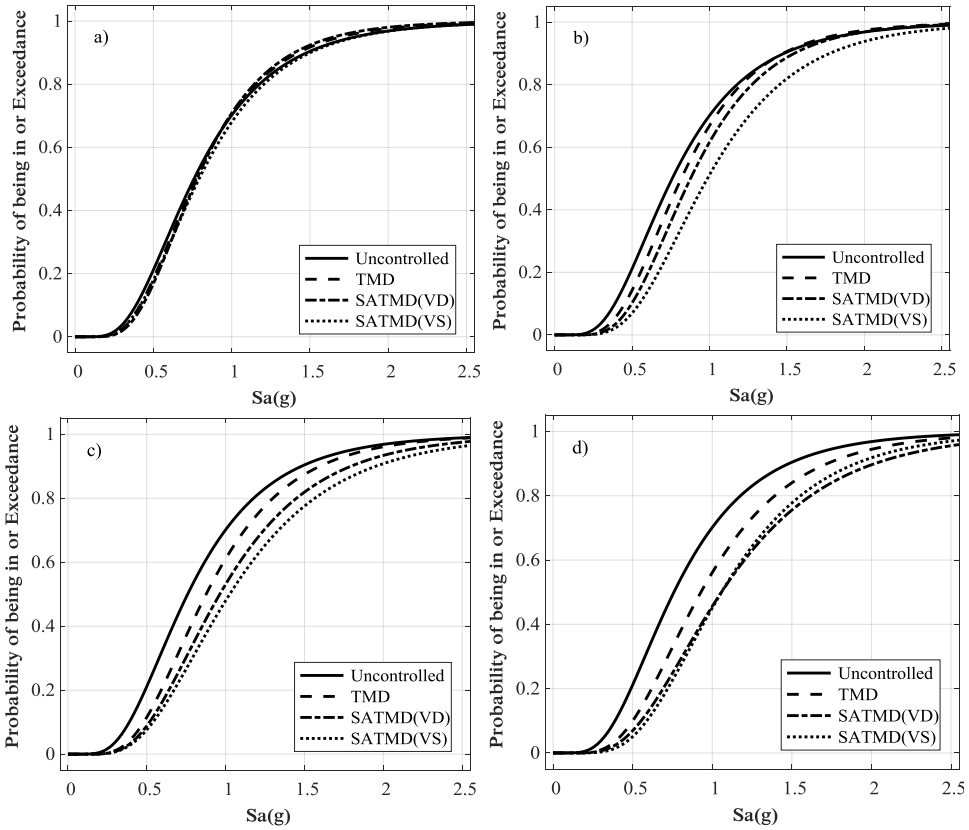

Figure 11. Fragility curves of uncontrolled structure and controlled with TMD and optimal SATMDs with mass ratio of a) μ=1%, b) μ=5%, c) μ=10% and d) μ=15% for LS performance level

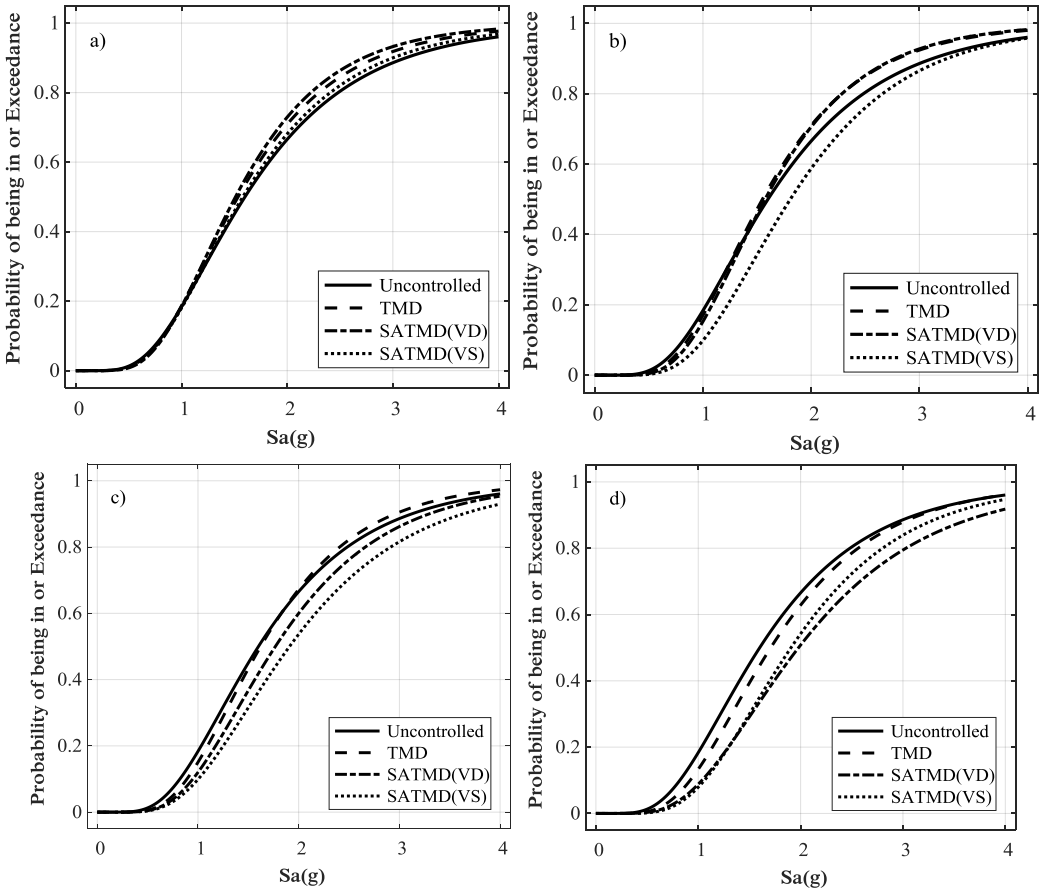

Figure 12. Fragility curves of uncontrolled structure and controlled with TMD and optimal SATMDs with mass ratio of a) μ=1%, b) μ=5%, c) μ=10% and d) μ=15% for CP performance level

6. CONCLUSIONS

This study deals with developing fragility curves for assessing the robustness of optimal variable damping and stiffness SATMDs on a nonlinear eight-story shear building. SATMDs with mass ratios of μ=1%,5%,10% and 15% have been designed based on an optimization technique with the objective function of minimization of maximum inter-story drift ratio as safety criterion which genetic algorithm has been used to solve the optimization problem. Uncertainty of the applied excitation has been considered by using 20 earthquake records and fragility curves of the structure equipped with optimal SATMDs have been developed and compared with the fragility curves of the uncontrolled structure and controlled structure using TMD. Numerical results show that in most range of intensity measure, especially IO and LS performance levels, using variable damping or stiffness SATMDs has enhanced seismic fragility of the structure and have the capability of improving reliability of the structure. Also, it has been found that increasing the mass ratio of the SATMDs has led to more enhancement on fragility of the structures. As an example,

variable stiffness SATMD with mass ratio of μ=15% has increased reliability of the structure about 20%, 25% and 15% with respect to the uncontrolled structure for IO, LS and CP performance level, respectively at Sa=0.5g, 1g and 1.5g. Comparing fragility curves of variable damping and stiffness SATMDs shows that similar to the design process, fragility curves of variable stiffness SATMD is less sensitive to the mass ratio than variable damping SATMD and by increasing the mass ratio both control systems perform almost similarly. For instance, at LS performance level and intensity measure of S_a=1.0g, variable stiffness SATMD with mass ratio of μ=5%,10% and 15% has increased the reliability of the structure about 19%, 22% and 25%, where variable damping SATMDs improved reliability about 8%, 17% and 24%, respectively. Also, it has been shown that SATMDs with variable damping and stiffness are more reliable than passive TMDs, especially, under severe earthquakes which the structure undergoes nonlinear behavior and TMDs are practically detuned. For example, at LS performance level and intensity measure of S_a=1.0g, variable stiffness SATMD with mass ratio of μ=5%,10% and 15% has increased the reliability of the structure about 16%, 13% and 10%, respectively in comparison with TMD.

REFERENCES

1. Arfiadi Y, Hadi MNS. Optimum placement and properties of tuned mass dampers using hybrid genetic algorithm, *Int J Optim Civil Eng* 2011; **1**(1): 167-87.
2. Farghali AA. Optimum design of TMD system for tall buildings, *Int J Optim Civil Eng* 2012; **2**(4): 511-32.
3. Mohebbi M, Alesh Nabidoust N. The capability of optimal single and multiple tuned mass dampers under multiple earthquakes, *Int J Optim Civil Eng* 2018; **8**(3): 469-88.
4. Pinkaew T, Fujino Y. Effectiveness of semi-active tuned mass dampers under harmonic excitation, *Eng Struct* 2001; **23**(7): 850-60.
5. Eason RP, Sun C, Nagarajaiah S, Dick AJ. Attenuation of a linear oscillator using a nonlinear and semi-active tuned mass damper in series, *J Sound Vib* 2013; **332**(1): 154-66.
6. Kaveh A, Pirgholizadeh S, Khadem Hosseini O. Semi-active tuned mass damper performance with optimized fuzzy controller using css algorithm, *Asian J Civil Eng* 2015; **16**(5): 587-606.
7. Sfahani MG, Guan H, Loo YC. Seismic reliability and risk assessment of structures based on fragility analysis – A review, *Adv Struct Eng* 2015; **18**(10): 1653-69.
8. Castaldo P, Amendola G, palazzo B. Seismic fragility and reliability of structures isolated by friction pendulum devices: seismic reliability-based design (SRBD), *Earthq Eng Struct Dyn* 2017; **46**(3): 425-46.
9. Wilbee AK, Pena F, Condori J, Sun Z, Dyke SJ. Fragility analysis of structures incorporating control systems, *6th International Conference on Advanced in Experimental Structural Engineering*, University of Illinois, Urbana-Champaign, United States, 2015.
10. Wong KKF, Harris JL. Seismic damage and fragility analysis of structures with tuned mass dampers based on plastic energy, *Struct Des Tall Special Build* 2012; **21**(4): 296-310.
11. Taylor E. The Development of Fragility Relationships for Controlled Structures, Master's thesis, Washington University, St. Louis, 2007.

12. Barnawi W. Seismic Fragility Relationships for Civil Structures Retrofitted with Semi-Active Devices, Master's thesis, Washington University, St. Louis, 2008.
13. Barnawi W, Dyke SJ. Fragility based analysis of a 20-story benchmark building with smart devices implementation, *Proceeding of the 11th Aerospace Division International Conference on Engineering*, Long Beach, CA, 2008.
14. Cha YJ, Bai JW. Seismic fragility estimates of controlled high-rise buildings with magnetorheological dampers, *Tenth U.S. National Conference on Earthquake Engineering*, Anchorage, Alaska, 2014.
15. Mohebbi M, Dabbagh HR, Moradpour S, Shakeri K, Tarbali K. DGA-based approach for optimal design of active mass damper for nonlinear structures considering ground motion effect, *Smart Mater Struct* 2015; **24**(4): 045017.
16. Newmark NM. A method of computing for structural dynamics, *J Eng Mech Div* 1959; **85**(3): 67-94.
17. Joghataie A, Mohebbi M. Optimal control of nonlinear frames by Newmak and distributed genetic algorithm, *Struct Des Tall Special Build* 2012; **21**(2): 77-95.
18. Holland JH. *Adaptation in Natural and Artificial Systems*, Ann Arbor: The University of Michigan Press, 1975.
19. Moradi M, Bagherieh AR, Esfahani MR. Damage and plasticity of conventional and high - strength concrete part1: statistical optimization using genetic algorithm, *Int J Optim Civil Eng* 2018; **8**(1): 77-99.
20. Gholizadeh S, Kamyab R, Dadashi H. Performance-based design optimization of steel moment frames, *Int J Optim Civil Eng* 2013; **3**(2): 327-43.
21. Biabani Hamedani K, Kalatjari VR. Structural system reliability-based optimization of truss structures using genetic algorithm, *Int J Optim Civil Eng* 2018; **8**(4): 565-86.
22. Mohebbi M, Moradpour S, Ghanbarpour Y. Improving the seismic behavior of nonlinear steel sructures using optimal MTMDs, *Int J Optim Civil Eng* 2014; **4**(1): 137-50.
23. Mohebbi M, Bagherkhani A. Optimal design of Maneto-Rheological Dampers, *Int J Optim Civil Eng* 2014; **4**(3): 361-80.
24. Mohebbi M, Dadkhah H. Optimal smart isolation system for multiple earthquakes, *Int J Optim Civil Eng* 2019; **9**(1): 19-37.
25. Goldberg DE. *Genetic Algorithms in Search, Optimization and Machine Learning*, Reading MA: Addison-Wesley, 1989.
26. Baker JE. Reducing bias and inefficiency in the selection algorithm, *Proceeding of the 2nd International Conference on Genetic Algorithm (ICGA)*, Cambridge, MA, 1987.
27. Mühlenbein H, Schlierkamp-Voosen D. Predictive models for the breeder genetic algorithm: I. Continuous parameter optimization, *Evolut Comput* 1993; **1**(1): 25-49.
28. Sadek F, Mohraz B, Taylor AW, Chung RM. A method of estimating the parameters of tuned mass dampers for seismic applications, *Earthq Eng Struct Dyn* 1997; **26**(6): 617-35.